Published in final edited form as:
J Am Chem Soc. 2010 January 13; 132(1): 32–33. doi:10.1021/ja908775g.

One-Pot Nucleation, Growth, Morphogenesis, and Passivation of 1.4 nm Au Nanoparticles on Self-Assembled Rosette Nanotubes

Rahul Chhabra[†,‡], **Jesus G. Moralez**[†,‡], **Jose Raez**[†,‡], **Takeshi Yamazaki**[†,¶], **Jae-Young Cho**[†], **Andrew J. Myles**[†], **Andriy Kovalenko**[†,¶], and **Hicham Fenniri**[†,‡,*]

[†]National Institute for Nanotechnology (NINT-NRC), University of Alberta, 11421 Saskatchewan Drive, Edmonton, Alberta T6G 2M9, Canada

[‡]Department of Chemistry, University of Alberta, 11421 Saskatchewan Drive, Edmonton, Alberta T6G 2M9, Canada

[¶]Department of Mechanical Engineering, University of Alberta, 11421 Saskatchewan Drive, Edmonton, Alberta T6G 2M9, Canada

Abstract

A one-pot strategy for the nucleation, growth, morphogenesis and passivation of 1.4 nm Au nanoparticles (NPs) on self-assembled rosette nanotubes (RNTs) is described. TM-AFM, TEM, EDX, SAED were used to establish the structure and organization of this hybrid material. Notably, we have found that the Au NPs formed were nearly monodisperse clusters of Au_{55} (1.4-1.5 nm) nestled in pockets on the RNT surface.

The modification of biomolecules with metal-based nanoparticles (NP) is allowing us to create materials with exciting new properties for applications in medicine, molecular electronics, optics and catalysis.[1] Researchers have been able to perform electroless deposition of NP's on DNA,2 peptides complexes,3 polymers,4 and nanotubes such as the tobacco mosaic virus,5 peptide nanotubes,6 and DNA-based nanotubes.7 However, coverage of the organic structure was generally incomplete and the NP size distribution was relatively broad. Sequence-specific deposition of Ag and Au NPs on DNA has been previously achieved on fully stretched DNA molecules on silicon substrates.[8] In this case, nucleoprotein strands, composed of RecA proteins bound to a sequence specific DNA strand, acted as a negative resist and protected specific regions of DNA from metallization. This approach was indeed a great advancement in the control of selective metallization of DNA, however this type of control has not been achieved yet in synthetic self-assembled nanostructure. Here, we report a one-pot process for the site-specific nucleation, growth, morphogenesis, and passivation of 1.4 nm Au NPs on self-assembled rosette nanotubes (RNTs).

The RNTs are a new class of biocompatible materials obtained through the self-assembly of a synthetic DNA base analogue, the G^C motif. Mediated by intermolecular hydrogen bonding, six of the heteroaromatic G^C bases self-assemble in water to form a supermacrocycle maintained by 18 H-bonds (rosette). The resulting and substantially more hydrophobic rosettes then self-organize to produce a tubular stack with tunable dimensions and properties.[9] The RNTs used in this study were assembled from a heteroaromatic bicyclic twin G^C base (**1**,

*hicham.fenniri@nrc-cnrc.gc.ca.

Supporting Information Available: Experimental details and additional figures. This material is available free of charge via the Internet at http://pubs.acs.org.

Figure 1A), which upon self-assembly forms a twin rosette maintained by 36 H-bonds (Figure 1B), then a helical stack (Figure 1C).[9d]

To assemble the RNTs, **1** was dissolved in water (1 mM), heated for 20 min at 90°C in an oil bath, and aged at room temperature for 24 h to ensure complete self-assembly. This solution was diluted to 50 μM and a sample (5 μL) was deposited on freshly cleaved mica and imaged by tapping mode atomic force microscopy (TM-AFM) and scanning electron microscopy (SEM) (Figure 2). The AFM height profile of the RNTs was ~3 nm, which is significantly lower than the measured (4.0 ± 0.3 nm) and calculated (4.0 nm) outer diameter. As in earlier reports, this discrepancy was attributed to the compressibility of the RNTs under the AFM tip. [9d] Both TM-AFM and SEM images confirmed the formation several μm long RNTs.

To incorporate Au NPs on the self-assembled RNTs, we reasoned that the positively charged lysine side chains would coordinate to the negatively charged tetrachloroaurate ($AuCl_4^-$). Upon reduction with hydrazine (N_2H_4) each lysine site could then act as a nucleation point for the formation of Au NPs. Thus, the [**1**]:[$HAuCl_4$] ratio was optimized to maximize the loading of Au NPs on the surface of the RNTs. We found that a ratio 1:20 equivalents of [**1**]:[$HAuCl_4$] gave the desired outcome. Below this ratio, the loading was insufficient, and a higher ratio resulted in polydisperse Au aggregates (data not shown). For the same reason, we established experimentally that the molar ratio of [$HAuCl_4$]:[$N_2H_4.H_2O$] must be kept constant (10:1) to ensure narrow size distribution of Au NPs on RNT templates.

In a typical experiment, a solution of **1** in water (200 μL, 50 μM, pH ~ 5-6) was mixed with $HAuCl_4$ (2 μL, 0.1 M) and incubated in the dark for 24 h (final pH ~3). $N_2H_4.H_2O$ (2 μL, 0.01 M) was then added to the reaction mixture (final pH ~3). It was important to have excess $AuCl_4^-$ ions, as these ions aid in the colloidal stability of the newly formed Au NPs.[10] A statistical analysis of the particle diameter and interparticle distance by transmission electron microscopy (TEM) was carried out on several hundred Au NPs, which resulted in a mean diameter of 1.4 ± 0.2 nm and a mean interparticle distance of 3.8 ± 0.8 nm.

In an attempt to increase Au NP loading on the RNTs the concentration of **1** was increased from 50 μM to 1 mM while maintaining the same [**1**]:[$HAuCl_4$] and [$HAuCl_4$]:[$N_2H_4.H_2O$] ratios. Addition of $HAuCl_4$ resulted in a pH drop from 3.5 to 1.7, which remained constant after addition of $N_2H_4.H_2O$. In this case the mean NP diameter was found to be 1.5 ± 0.1 nm with interparticle distance of 3.5 ± 0.4 nm. The similarity of Au NPs size was attributed to the templating effect of the RNTs (*vide infra*). TM–AFM of this sample showed the formation of rigid thread-like structures with a height of ~ 4.6 nm (Figure 3A) in excellent agreement with the calculated diameter of the Au NPs/RNT composite (Figure S8). TEM analysis unambiguously established the RNTs' ability to nucleate and template the growth and morphogenesis of the Au NPs that appear as small dots on the RNTs surface (Figure 3B). Their size distribution is remarkably low relative to previously reported systems.[11] Furthermore, the size of 1.4-1.5 nm suggests that these NPs are likely Schmid's clusters (Au_{55}).[12] To further confirm this hypothesis, energydispersive X-ray (EDX) analysis and selected area electron diffraction were carried out (Figures S2, S3).

Analysis of the organization of the Au NPs on several TEM images revealed a helical arrangement on the RNTs at an angle of 40.1 ± 2.3° (Figure 3B inset, Figure S8), whereas the closest distance between Au NPs along the long axis of the RNT was 3.5 ± 0.3 nm (distance between blue lines in Figure 3B inset) and 4.2 ± 0.3 across the RNT (wall to wall distance). Based on these observations, the model in Figure 1D-F was built. This model shows pockets of 1.6 nm in cross section defined by 4 adjacent lysine side chains (Figure 1F) that could accommodate a 1.4-1.5 nm Au NP. The next available pocket along the main axis of the RNT is 1.4–1.6 nm away, thus resulting in an interparticle distance of ~3.2 nm (Figure S8). However,

at a ±20° angle on each side of each pocket additional nucelation site are available, accounting for the angular relationship between Au NPs.

A statistical analysis of the TEM images revealed that out of the maximum number of sites (188 sites/100 nm) only ~30% were filled (58 sites/100 nm). Figure S8 (A, B) shows two models, a theoretical maximum occupancy model (A) and a zigzag model based on TEM measurements. The zigzag model not only accounts for the ~30% loading and interparticle distances measured, but it also reduces interparticle repulsion as each nucleation site is surrounded with four unoccupied sites. The open version of the maximum occupancy and zigzag models are shown in Figure S8 (C, D).

Since the majority of the Au NPs are located on the RNTs, we believe that the low loading is either due to (a) electrostatic repulsion between Au NPs, or (b) incomplete loading due to limited supply of reducing agent (limiting reagent in this system). To test the second hypothesis, we added excess hydrazine (10 and 100 equivalents relative to **1**) but this resulted in the formation of large polydisperse particles without improving the RNT loading. Therefore we believe that the maximum loading of this particular RNT cannot exceed ~30% most likely for electrostatic reasons.

Each nucleation pocket is composed of four adjacent lysine side chains wherein each lysine could accommodate 3 $AuCl_4^-$ ions correlating with the protonation states of the lysine side chain (Figure 1A). Thus, taking into consideration the zigzag model (~30% occupancy with Au_{55} NP) each equivalent of molecule **1** will require ~4.1 equivalents of Au(III) and 6.2 equivalents of N_2H_4 (that is 3 mole equivalents of N_2H_4 for every 2 mole equivalents of Au (III)). Experimentally, we used 20 equivalents of Au(III) (i.e. ~5 fold excess for the zigzag model), but only 2 equivalents of N_2H_4 relative to compound **1** (i.e. ~3 fold below what is needed for the conversion of all RNTs to the zigzag model). Based on this estimate, one should expect the distribution of Au NP on the RNTs to be less dense, which leads us to speculate that a significant proportion of RNTs that aggregate in the presence of excess $AuCl_4^-$ ions did not get exposed to N_2H_4.

In conclusion, we have demonstrated that self-assembled RNTs can be used to nuclate nearly monodisperse Au NPs. Future studies include the nucleation of other metal nanopartilces for applications in catalysis, nanoelectronics, and nanophotonics.

Supplementary Material

Refer to Web version on PubMed Central for supplementary material.

Acknowledgments

We thank NIH (NIH EB03824), NSERC, NRC and the University of Alberta for supporting this program. JGM thanks NIH (GM55146-08) for a graduate fellowship.

References

(1) (a). Daniel M-C, Astruc D. Chem. Rev 2004;104:293–346. [PubMed: 14719978] (b) Rosi NL, Mirkin CA. Chem. Rev 2005;105:1547–1562. [PubMed: 15826019]

(2). Yan H, Park SH, Finkelstein G, Reif JH, LaBean TH. Science 2003;301:1882–1884. [PubMed: 14512621]

(3). Chen C-L, Zhang P, Rosi NL. J. Am. Chem. Soc 2008;130:13555–13557. [PubMed: 18800838]

(4). Ofir Y, Samanta B, Rotello VM. Chem. Soc. Rev 2008;37:1814–1825. [PubMed: 18762831]

(5). Knez M, Bittner AM, Boesm F, Wege C, Jeske H, Maiß E, Kern K. Nano Lett 2003;3:1079–1082.

(6). Carny O, Shalev DE, Gazit E. Nano Lett 2006;6:1594–1597. [PubMed: 16895341]

(7) (a). Liu D, Park SH, Reif JH, LaBean TH. Proc. Natl. Acad. Sci. USA 2004;101:717–722. [PubMed: 14709674] (b) Sharma J, Chhabra R, Cheng A, Brownell J, Liu Y, Yan H. Science 2009;323:112–116. [PubMed: 19119229]

(8). Keren K, Krueger M, Gilad R, Ben-Yoseph G, Sivan U, Braun E. Science 2002;297:72–75. [PubMed: 12098693]

(9) (a). Fenniri H, Mathivanan P, Vidale KL, Sherman DM, Hallenga K, Wood KV, Stowell JG. J. Am. Chem. Soc 2001;123:3854–3855. [PubMed: 11457132] (b) Fenniri H, Deng B-L, Ribbe AE. J. Am. Chem. Soc 2002;124:11064–11072. [PubMed: 12224954] (c) Chun A, Moralez JG, Fenniri H, Webster TJ. Nanotechnology 2004;15:S234–S239. (d) Moralez JG, Raez J, Yamazaki T, Motkuri RK, Kovalenko A, Fenniri H. J. Am. Chem. Soc 2005;127:8307–8309. [PubMed: 15941263]

(10). Pei L, Mori K, Adachi M. Langmuir 2004;20:7837–7843. [PubMed: 15323538]

(11). Djalali R, Chen Y, Matsui H. J. Am. Chem. Soc 2002;124:13660–13661. [PubMed: 12431080]

(12). Schmid G. Chem. Rev 1992;92:1709–1727.

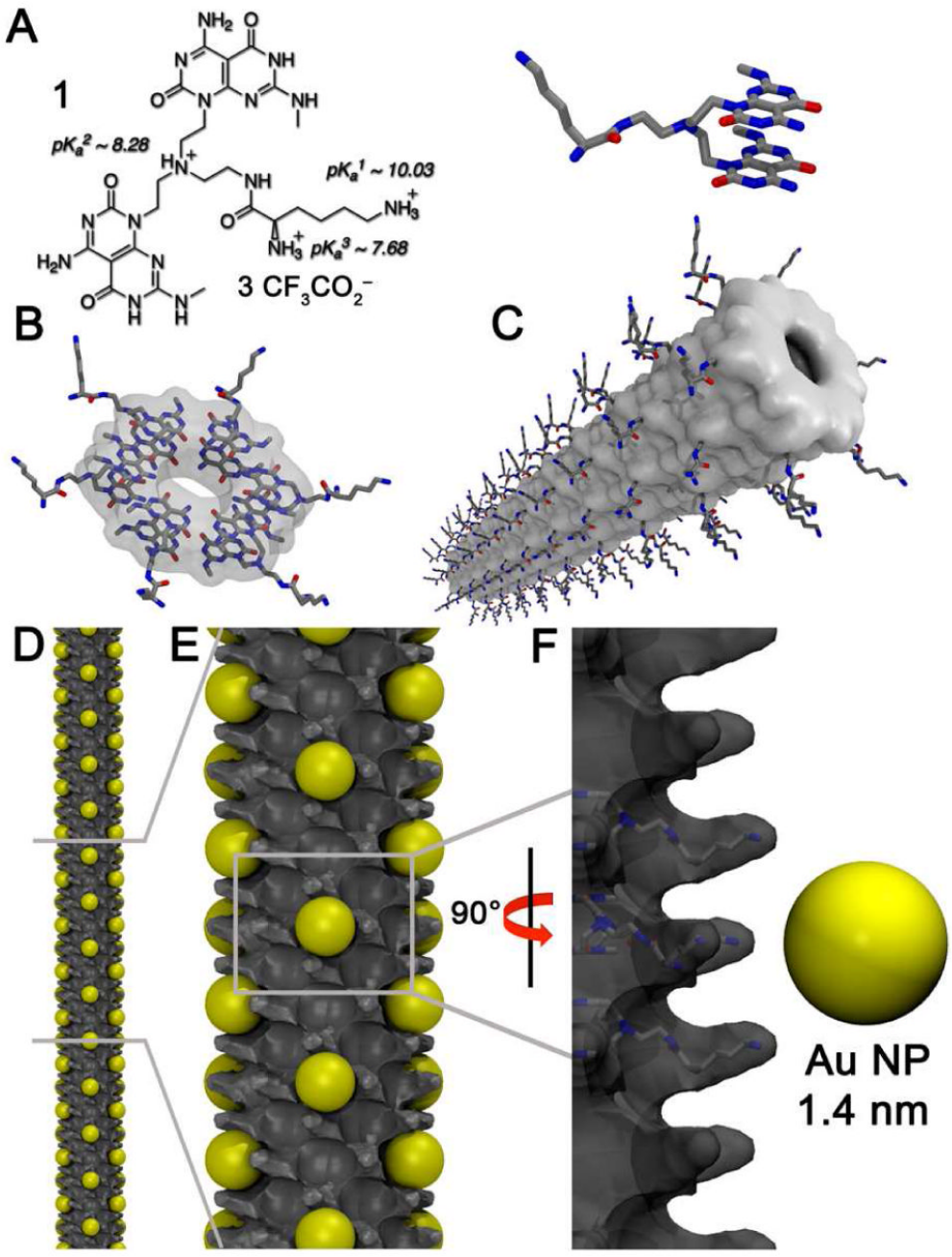

Figure 1.
Schematic of the RNTs as nucleation templates. (A) Twin G^C base (**1**), (B) self-assembled rosette, (C) self-assembled RNT obtained from rosette stacking, (D and E) RNTs with nucleated Au NPs (gold spheres), (F) close up view of the nucleation site.

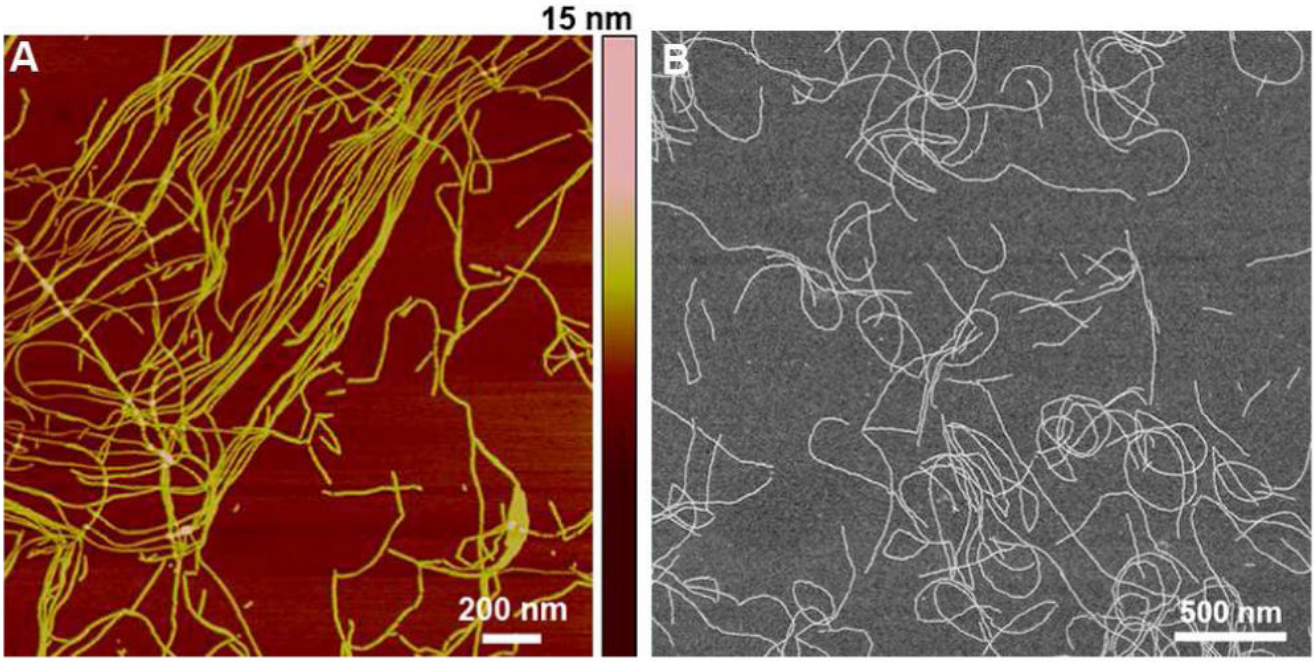

Figure 2.
TM-AFM image of RNTs on mica (A) and SEM micrographs of the same sample on a carbon-coated copper grid.

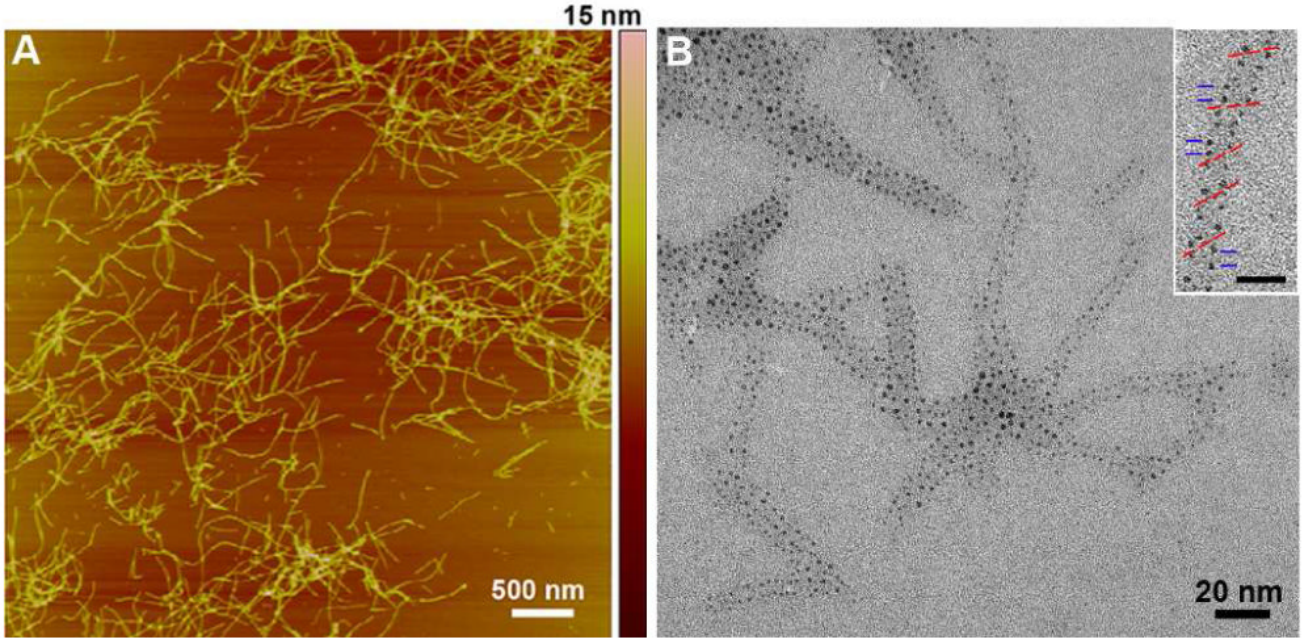

Figure 3.
TM-AFM image of the Au NPs coated RNTs on mica (A) and TEM image showing monodisperse Au NP/RNT composite on carbon coated grid. The inset shows a helical organization of Au NPs on RNT templates where the red lines indicate the pitch angle and the blue lines indicate the distance between adjacent Au NPs (scale bar = 10 nm).